Suppression of weak antilocalization in InAs nanowires

P. Roulleau,[1] T. Choi,[1] S. Riedi,[1] T. Heinzel,[2] I. Shorubalko,[1,3] T. Ihn,[1] and K. Ensslin[1]
[1]*Solid State Physics Laboratory, ETH Zurich, 8093 Zurich, Switzerland*
[2]*Condensed Matter Physics Laboratory, Heinrich-Heine-Universität, Universitätsstrasse 1, 40225 Düsseldorf, Germany*
[3]*Electronics/Metrology/Reliability Laboratory, EMPA, 8600 Dübendorf, Switzerland*
(Received 12 January 2010; revised manuscript received 30 March 2010; published 23 April 2010)

We investigate the crossover between weak localization and weak antilocalization in InAs nanowires of different diameters (75 nm-140 nm-217 nm). For a magnetic field applied perpendicularly to the nanowire axis, we extract the spin orbit and coherence lengths using a quasi-one-dimensional model of the conductance. We find a spin-orbit length inversely proportional to the width of the nanowire. When a parallel magnetic field is applied, we observe that the weak-antilocalization contribution is less affected by the magnetic field than in the perpendicular case.

DOI: 10.1103/PhysRevB.81.155449 PACS number(s): 62.23.Hj, 85.35.−p, 73.63.−b, 71.70.Ej

Electrons in InAs nanowires (NWs) have a relatively small effective mass $m^\star=0.023m_0$ (with m_0 the free-electron mass) and large electronic $g^\star$ factor leading to weak carrier-carrier interactions and strong spin-orbit interactions. The elastic mean-free path in InAs nanowires is small (~30 nm) compared to the wire length L and the diameter D, making transport for experiments mostly diffusive. For bulk InAs the Fermi level is known to be pinned at the surface in the conduction band leading to a surface accumulation layer of electrons even without gating or additional doping. For InAs nanowires the radial charge distribution is unknown. Experimentally it has been found that the wires stop to conduct at low temperatures below diameters of about 50 nm.[1] The charge distribution as well as scattering potentials and spin-orbit interactions can be investigated by magnetotransport experiments focusing on the low magnetic field regime, where universal conductance fluctuations (UCF), weak-localization (WL), and weak-antilocalization (WAL) effects become relevant. This regime has been investigated previously with 45 wires being measured in parallel.[2] This leads to averaging of the signal arising from UCF and allows the investigation of the crossover from weak localization to weak antilocalization. More recently,[3] it has been shown that it is possible to study this crossover by measuring electron transport through individual nanowires. This approach offers the possibility to understand the influence of the nanowire diameter and magnetic field orientation on the low-field correction of the conductivity.

In our experiment, we study the magnetotransport properties of individual nanowires for different back-gate voltages. We extract the phase coherence length l_φ and the spin-orbit interaction length l_{SO} and tune them with the back gate: for $l_\varphi<l_{SO}$ we observe the WL correction of the conductivity, whereas for $l_\varphi>l_{SO}$ the correction of the conductivity is due to WAL. Our measured values of l_φ and l_{SO} are in good agreement with previous experiments. We reproduce these measurements for nanowires of different diameters and find a diameter dependence of the correction of the conductivity. We explain this dependence considering spin precession induced by the presence of Rashba spin splitting and the confinement of electronic orbitals in the nanowire. We finally discuss the influence of the magnetic field orientation.

We grow InAs NWs on $\langle 111\rangle B$ oriented GaAs substrates by metal-organic vapor phase epitaxy.[4,5] The growth process is catalyzed by monodisperse colloidal Au particles with diameters of 40 nm. The resulting NWs are between 5 and 10 μm long and have diameters between 75 and 220 nm. Here we present data for three nanowires of different widths covering the accessible range. The NWs are then transferred to a highly doped Si substrate which can be used as a back gate covered by 300 nm of SiO_2. Optical lithography is used to contact the nanowires by evaporation of Ti/Au giving a typical contact spacing of ≈1.7 μm (inset of Fig. 1). The low contact resistance[1,6] (less than 100 Ω) enables us to use a two-point measurement configuration. Electrical measurements were performed at 2 K, and a revolving chip carrier is used to vary the angle between the axis of the nanowire and the applied magnetic field. We first discuss the configuration when the applied magnetic field is perpendicular to the nanowire axis.

The result of our magnetotransport study for the thin nanowire (75 nm) is shown in Fig. 1 in a small magnetic field range and for different back-gate voltages. The symme-

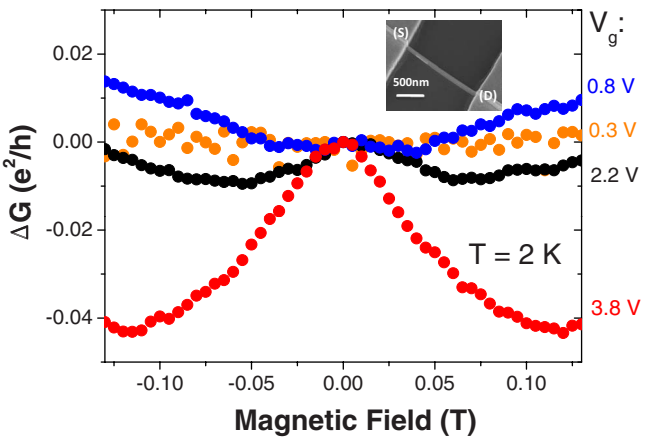

FIG. 1. (Color online) Magnetoconductance, offset to zero at zero magnetic field, at a temperature of 2 K plotted for four different gate voltages. The WAL peak is clearly visible at high back-gate voltages, despite the presence of conductance fluctuations due to the short elastic-scattering length. Inset: scanning electron micrograph of a device similar to the one measured. Source (S) and drain (D) ohmic contacts to the NW are defined by optical lithography.

 ©2010 The American Physical Society

try in magnetic field confirms that the measurements are in the linear transport regime. We observe an enhancement of the WAL correction when the back-gate voltage is increased, despite conductance fluctuations due to a short elastic-scattering length. To clarify the crossover from WL to WAL, we smoothen our conductance measurements by averaging curves taken in a small range of back-gate voltages as described below: indeed contrary to the Dhara *et al.*[3] experiment, conductance fluctuations prevent us from extracting the spin-orbit length l_{SO} and the coherence length l_φ before averaging.

In order to smoothen the fluctuations, we first calculate the autocorrelation function[7]

$$F(\Delta V_{bg}) = \langle \delta G(V_{bg} + \Delta V_{bg}) \delta G(V_{bg}) \rangle_{V_{bg}},$$

where $\delta G(V_{bg})$ is the conductance as a function of V_{bg} with the average subtracted and $\langle \cdots \rangle_{V_{bg}}$ denotes the average over V_{bg}. The back-gate voltage corresponding to half the maximum of the autocorrelation function $F(V_{bg}^c) = \frac{1}{2}F(0)$ defines the correlation voltage V_{bg}^c. We find $V_{bg}^c \sim 1$ V. Thus, we average over a range of 2 V in back-gate voltage.

In Fig. 2(a) we present such smoothed curves for different back-gate voltages: we first notice a transition from a WL dip for small V_{bg} to a WAL peak for larger values. To characterize this transition, we consider a quasi-one-dimensional model which assumes $L \gg l_\varphi \gg D \gg \lambda_F$ (where L is the length of the nanowire and D its diameter). The elastic-scattering time $\tau_{el} = \mu m^*/e$, as well as the corresponding elastic mean-free path $l_{el} = \nu_F \tau_{el}$ (with ν_F the Fermi velocity) were extracted from the mobility[8] and the electron concentration of the wires. Since in our case the mobility is $\mu \sim 1500$ cm^2/V s and the electron concentration $n \sim 10^{18}$ cm^{-3}, the elastic-scattering length can be estimated to be around $l_e \sim 30$ nm which corresponds to the so-called dirty metal limit.[9] We therefore fit according to the theory of the dirty metal regime ($l_e \ll D$) rather than the pure limit ($l_e \gg D$). The correction of the conductance $\Delta G(B)$ is then given by[10,11]

$$\Delta G(B) = -\frac{2e^2}{hL}\left[\frac{3}{2}\left(\frac{1}{l_\varphi^2} + \frac{4}{3l_{SO}^2} + \frac{1}{D_c \tau_B}\right)^{-1/2} - \frac{1}{2}\left(\frac{1}{l_\varphi^2} + \frac{1}{D_c \tau_B}\right)^{-1/2}\right] \quad (1)$$

[represented by solid lines in Fig. 2(a)] with D_c being the diffusion constant and τ_B the magnetic relaxation time. It can be seen that the curves obtained using the least mean-square method do not fit the data perfectly well. Alternatively we have deduced l_φ from the curvature of $\Delta G(B)$ at low B and l_{SO} from the position of the minimum in $\Delta G(B)$ and find agreement with the least mean-square method within 10%. Therefore, we will continue using the least mean-square method in the remainder of the paper. Fitting parameters are the spin-orbit length l_{SO} and the coherence length l_φ shown as a function of the back-gate voltage [in Fig. 2(b)]. For $V_{bg} < 1$ V, $l_\varphi < l_{SO}$ the conductance correction is predominately due to WL and for $V_{bg} > 1$ V, $l_\varphi > l_{SO}$ the conductance correction is predominately due to WAL.

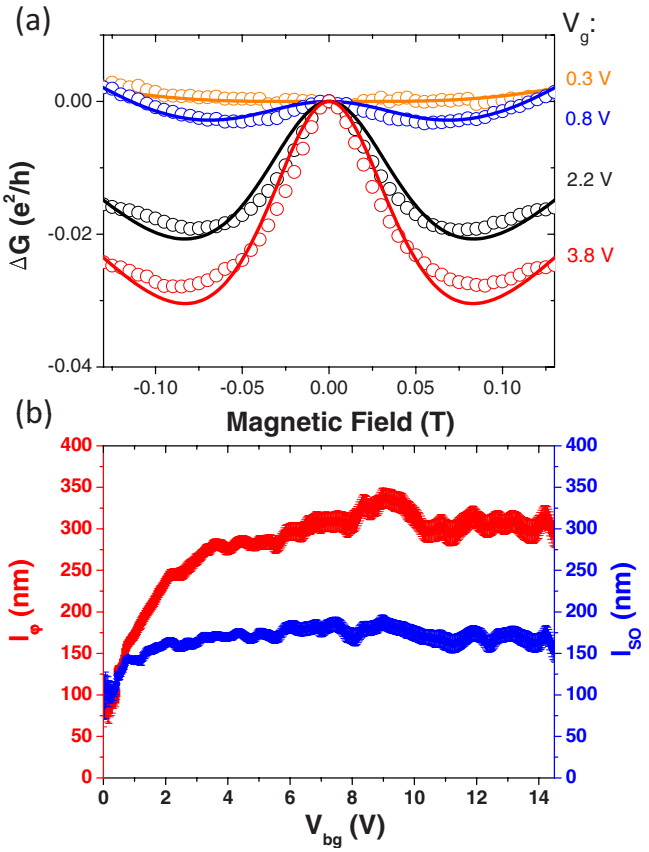

FIG. 2. (Color online) (a) In dots: correction of the conductance for different back gates. In order to smooth fluctuations, each curve has been averaged over a range of 2 V back gate. A crossover from WL to WAL is observed when the back-gate voltage is increased. Solid lines: fits using formula (1), (b) extracted spin orbit l_{SO} and coherence length l_φ as a function of the back-gate voltage. At $V_{bg} \sim 1$ V, l_φ becomes larger than l_{SO}: this crossover indicates the transition from WL to WAL.

We compare our results for the WAL/WL crossover with those obtained by other groups. Hansen *et al.*[2] who have studied an ensemble of 45 InAs NWs (diameter $D = 60 \pm 4$ nm) measured in parallel, have extracted $l_\varphi \sim 240$ nm and $l_{SO} \sim 150$ nm for large back-gate voltages in the dirty limit and at 8 K. More recently, Dhara *et al.*[3] have observed a similar crossover for a single and thicker ($D = 90$ nm) nanowire: for large back-gate voltages they extract a smaller $l_{SO} \sim 100$ nm. We will show below that we also measure a smaller l_{SO} when the nanowire is thicker.

Up to now, we presented results obtained on a $D = 75$ nm nanowire. We have also performed similar measurements for $D = 140$ nm and $D = 217$ nm nanowires and find a strong diameter dependence of the spin-orbit length. Figure 3 shows the spin-orbit length as a function of back-gate voltage for the three different diameters. When the nanowire gets thicker, the extracted spin-orbit length is smaller. To discuss the diameter dependence, we plot (inset of Fig. 3) the average l_{SO} versus back-gate voltage as a function of the diameter and observe a decrease which is compatible with a $\sim 1/D$ behavior (with D the diameter of the wire).

A similar width dependence has already been reported for

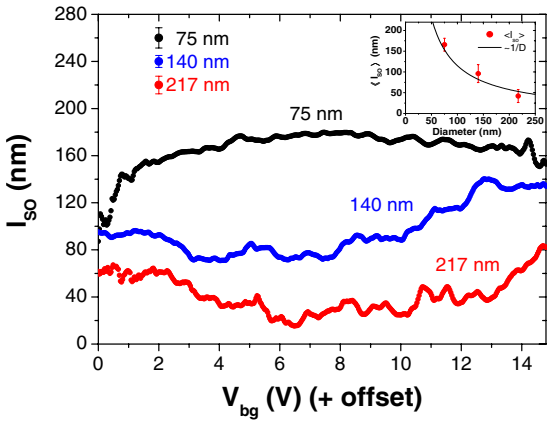

FIG. 3. (Color online) Comparison of the back-gate voltage dependence of l_{SO} for three different NW diameters (75 nm in black, 140 nm in blue, and 217 nm in red). Each curve has been averaged over a range of 5 V in back-gate voltage and fitting is restricted to $|B| \leq 150$ mT. The pinch-off voltage is set to 0 for all three curves. Inset: averaged spin-orbit length as a function of the wire diameter. The red filled dots indicate the arithmetic mean for each l_{SO} curve in Fig. 3. Fitting the data (black solid line) confirms that l_{SO} is compatible with a D^{-1} dependence.

$Ga_xIn_{1-x}As/InP$ narrow quantum wires:[12] a crossover from WAL to WL is observed as the wire width is reduced. To explain this observation, Schäpers *et al.* showed that this effect arises from a width-dependent wire confinement and not from a change in the Rashba coupling:[13] in other words, this effect is purely geometrical. Inspired by the width dependence of the magnetic dephasing length in wires,[9] they find in the *dirty metal* regime ($l_e \ll D$),

$$l_{SO} = \frac{\sqrt{3} l_R^2}{D} \tag{2}$$

with l_R the ballistic spin-precession length $l_R = \hbar^2/(2m^*\alpha_R)$ and α_R the Rashba coupling parameter. In our case, the microscopic origin of zero-field spin splitting could be a structural asymmetry in radial direction, represented by an effective (Rashba-type) electric field pointing radially away from the wire axis. Since we do not have any direct way to extract this Rashba coupling, we will assume that it remains the same in the three wires.[14] Depending on the sign of this electric field, this could lead to states localized around the wire axis or to surface states that wrap around the wire at a finite radius. In the latter case, we would expect to find Aharonov-Bohm oscillations for a magnetic field parallel to the axis of the nanowire which we did not observe. We will assume then that the bound state is localized close to the wire axis. This is in agreement with the fact that these nanowires do not conduct for small diameters.[1] In Fig. 3 (inset), we fit the average spin-orbit length with the expected diameter dependence given by formula (2) and extract a spin-precession length $l_R \sim 81$ nm. Since l_R is related to α_R via $l_R = \hbar^2/(2m^*\alpha_R)$, we obtain a coupling parameter equal to $\alpha_R = 2 \times 10^{-11}$ eV m in reasonable agreement with other experiments realized in bulk InAs for a 2D electron gas (2DEG)

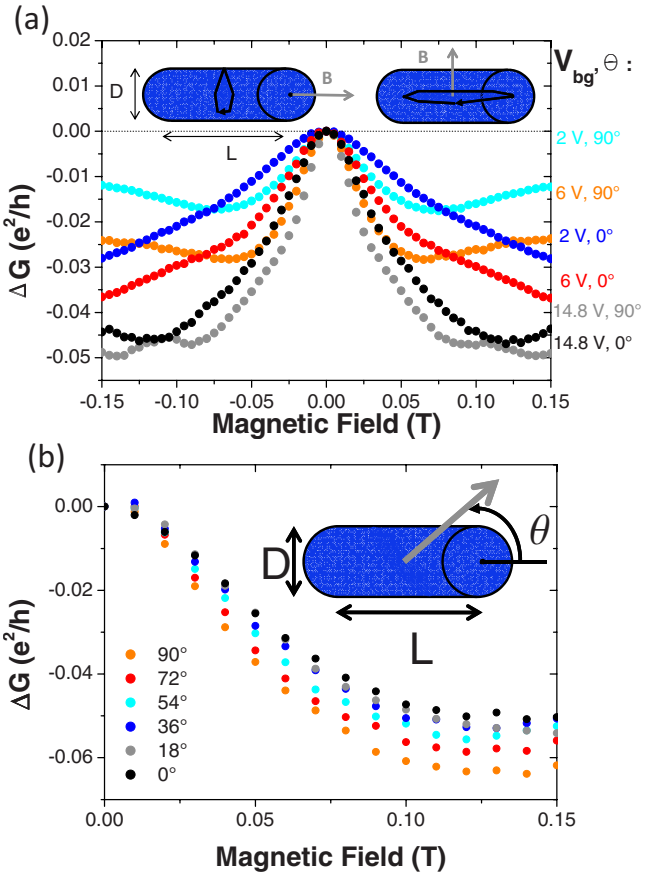

FIG. 4. (Color online) (a) Comparison of the magnetoconductance (smoothed over $\Delta V_{bg} = 2$ V), measured at perpendicular ($\theta = 90°$) and parallel ($\theta = 0°$) magnetic field for the 75-nm-wide nanowire. The WAL peak is wider in the parallel configuration (for all measured V_{bg} values). Additionally, the position of the first minimum is lower in the parallel case. Inset (left): example of a relevant closed path in the parallel magnetic field case. (Right): perpendicular magnetic field case. (b) Dependence of the WAL peak width as a function of the angle between the nanowire axis and the applied magnetic field (each curve is averaged around $V_{bg} = 12$ V. Only half of the peak is shown). A continuous transition from $\theta = 0°$ (parallel alignment) to $\theta = 90°$ (perpendicular alignment) is visible. Inset: scheme to clarify the definition of the angle θ.

forming at the surface of a bulk InAs crystal where $\alpha_R \sim 1 \times 10^{-11}$ eV m has been reported.[15]

Other mechanisms could also lead to a WAL correction of the conductivity. Hansen *et al.*[2] also discuss the Dresselhaus effect.[16] However, this effect, which depends on bulk-induced asymmetry, should not contribute because of the absence of spin splitting in the direction of transport ($\langle 111 \rangle$).[17]

We next consider the dependence of WAL correction on the magnetic field orientation. We can pass continuously from a perpendicular to a parallel magnetic field configuration since our samples are mounted on a revolving sample holder.

In Fig. 4(a) we represent the WAL correction of the 75-nm-diameter nanowire for three different back-gate voltages. We notice a significantly wider peak for parallel magnetic field compared to the perpendicular magnetic field case. In addition, the position of the first minimum is considerably

lower in $\Delta G(B)$ in the parallel case. The observed difference in the peak width leads to the question whether there is a continuous transition if we change the orientation of the sample relative to the magnetic field from perpendicular to parallel. In Fig. 4(b), we show the WAL correction for intermediate values of the angle between the wire axis and the applied magnetic field. We observe a continuous transition from $\theta=0°$ (parallel) to $\theta=90°$ (perpendicular) alignment. To understand this evolution, we must consider the electronic trajectories responsible for the correction in both cases. All pairs of time reversed paths participate in the magnetotransport correction. This correction is maximal at zero magnetic field but at finite magnetic field back-scattering paths with sufficiently large area such that they are penetrated by magnetic flux at least of the order of the magnetic-flux quantum will drop out of the quantum correction to the conductance. For a perpendicular magnetic field, the shape of the relevant closed paths can be arbitrarily elongated along the wire axis [see Fig. 4(a) inset]. Time-reversed paths enclosing an area extended over the entire cross section with no length restriction along the wire will be strongly affected by the magnetic field. In the parallel magnetic field case, we first have to evaluate the number of bound states quantized in the transverse direction that will participate in the WAL correction. A rough estimation for a 75 nm nanowire thickness, with $\lambda_F \sim 15$ nm, gives N the number of available states $\pi D/\lambda_F \sim 16$. Contrary to the perpendicular configuration, only very few backscattering paths will enclose an area large enough to be penetrated by a magnetic flux of at least the order of the magnetic-flux quantum: the effect of the magnetic field is expected to be less important, and the WAL peak wider, as observed experimentally.

In conclusion, we have observed a WL-WAL crossover of the quantum correction of the conductivity for single InAs nanowires. We have shown that this correction was strongly affected by the diameter of the nanowire and by the orientation of the applied magnetic field with respect to the nanowire axis. To explain the diameter dependence, we have considered the Rashba coupling and have shown that decreasing the diameter of the wire modifies the confinement and increases the spin-relaxation length. Similarly, when the applied magnetic field is parallel to the nanowire axis, the confinement is stronger and the WAL correction is less affected by the magnetic field.

We thank U. Zülicke for stimulating discussions and E. Gini for advice in nanowire growth. We acknowledge financial support from the ETH Zurich, the Swiss Science Foundation (SNF) and by EU Spico.

[1] A. Pfund, I. Shorubalko, R. Leturcq, M. T. Borgström, F. Grammand, E. Müller, and K. Ensslin, Chimia **60**, 729 (2006).
[2] A. E. Hansen, M. T. Björk, I. C. Fasth, C. Thelander, and L. Samuelson, Phys. Rev. B **71**, 205328 (2005).
[3] S. Dhara, H. S. Solanki, V. Singh, A. Narayanan, P. Chaudhari, M. Gokhale, A. Bhattacharya, and M. M. Deshmukh, Phys. Rev. B **79**, 121311(R) (2009).
[4] K. Hiruma, M. Yazawa, T. Katsuyama, K. Ogawa, K. Haraguchi, M. Koguchi, and H. Kakibayashi, J. Appl. Phys. **77**, 447 (1995).
[5] W. Seifert *et al.*, J. Cryst. Growth **272**, 211 (2004).
[6] H. Oigawa, J.-F. Fan, Y. Nannichi, H. Sugahara, and M. Oshima, Jpn. J. Appl. Phys. **30**, L322 (1991).
[7] G. Petersen, S. E. Hernández, R. Calarco, N. Demarina, and Th. Schäpers, Phys. Rev. B **80**, 125321 (2009).
[8] A. C. Ford, J. C. Ho, Y.-L. Chueh, Y.-C. Tseng, Z. Fan, J. Guo, J. Bokor, and A. Javey, Nano Lett. **9**, 360 (2009).
[9] C. W. J. Beenakker and H. van Houten, Phys. Rev. B **38**, 3232 (1988).
[10] B. L. Altshuler and A. G. Aronov, JETP Lett. **33**, 499 (1981).
[11] C. Kurdak, A. M. Chang, A. Chin, and T. Y. Chang, Phys. Rev. B **46**, 6846 (1992).
[12] Th. Schäpers, V. A. Guzenko, M. G. Pala, U. Zülicke, M. Governale, J. Knobbe, and H. Hardtdegen, Phys. Rev. B **74**, 081301(R) (2006).
[13] Y. L. L. Bychkov and E. Rashba, J. Phys. C **17**, 6039 (1984).
[14] V. A. Guzenko, J. Knobbe, H. Hardtdegen, T. Schäpers, and A. Bringer, Appl. Phys. Lett. **88**, 032102 (2006).
[15] T. Matsuyama, R. Kursten, C. Meissner, and U. Merkt, Phys. Rev. B **61**, 15588 (2000).
[16] G. Dresselhaus, Phys. Rev. **100**, 580 (1955).
[17] R. J. Elliott, Phys. Rev. **96**, 266 (1954).